COBEM 2021 26th International Congress of Mechanical Engineering
November 22-26, 2021, Virtual Congress, Brazil
ABCM Associação Brasileira de Engenharia e Ciências Mecânicas

# COB-2021-2332
# WAVE PROPAGATION IN A RAINBOW METAMATERIAL BEAM

**Fábio C. M. Oliveira**
**José Maria C. Dos Santos**
University of Campinas, UNICAMP-FEM-DMC, Rua Mendeleyev 200, Cidade Universitária Zeferino Vaz, Campinas - SP, Brazil.
fah_hc@hotmail.com, zema@unicamp.br

***Abstract.*** *Metamaterials and phononic crystals (PCs) are broadly investigated for noise and vibration attenuation due to the stop-bands generated by local resonance or Bragg effect, respectively. However, metamaterials and PCs application are limited by the stop-band widths. The recently established rainbow metamaterials, consisting of aperiodic graded arrays of resonators, are opening new possibilities to broadband control of propagation of mechanical waves, and to generate wider stop-bands than periodic structures. They are based on the rainbow trapping phenomena, which separates different frequency wave components and trap them in different positions in space. By modeling the elastic metamaterials to be graded in the unit cell distribution, robust elastic dispersion can be achieved and wave speed can be modulated to slow down to zero, and trapped in separate positions of space. Based on this approach, a rainbow metamaterial composed by a graded array of resonant beams attached transversely to a host longitudinal beam is proposed in the present study. To demonstrate the rainbow effects, a conventional periodic metamaterial and an aperiodic rainbow metamaterial are investigated. Both metamaterial designs are modeled by the Spectral Element (SE) method and the Finite Element (FE) method. The simulated results are compared to each other and the results showed that the aperiodic rainbow metamaterial beam has extended stop-bands compared with the periodic one. Others results related to the rainbow effects, like slowing down the elastic waves are also presented.*

***Keywords:*** *rainbow metamaterial, phononic crystals, stop-band, spectral element, finite element.*

## 1. INTRODUCTION

Metamaterials (MMs) and phononic crystals (PCs) are man-made artificial materials, broadly investigated due unusual properties such as negative effective mass, stiffness, and bulk modulus (Liu *et al.*, 2000; Fang *et al.*, 2006). Originally introduced to control optical waves (Pendry, 2020), the concept of MMs and PCs have expanded to the areas of acoustic and elastic metamaterials. These exotic properties are important for noise and vibration attenuation due the capacity to generate local resonance or Bragg effect stop-bands. However, MMs and PCs application have physical limitations to produce large stop-bands. Therefore, many elastic/acoustic PCs have been proposed by combining high contrast material properties and/or varied geometries (Assis *et al.*, 2019; Goto *et al.*, 2020; Fabro *et al.*, 2021). Also, periodic MMs with different types and arrangements of local resonators have been tried (Nobrega *et al.*, 2016; Miranda *et al.*, 2019; Xiao *et al.*, 2021). In general, most of these MMs and PCs are periodic systems and although these are relevant to control wave propagation and provide vibration/acoustic attenuation, large stop-bands are not easy to reached. In 1997, Brennan (1997) proposed an array of resonators with slightly different natural frequencies to attenuate vibration in a wide frequency band. More recently some works presented aperiodic MMs using graded local resonator, which can achieve better vibration attenuation (Hua *et al.*, 2021; Banerjee, 2021). Similarly, the rainbow metamaterial consisting of aperiodic graded arrays of resonators, are obtaining broadband control of wave propagation in mechanical systems, and generating wider stop-bands (D'Alessandro *et al.*, 2020; Meng *et al.*, 2020). Nevertheless, these approaches are at the beginning and needs to be studied systematically to produces optimal design procedures.

Based on this approach, a rainbow metamaterial composed by a graded array of resonant beams attached transversely to a host longitudinal beam is proposed in the present study. To demonstrate the rainbow effects, a conventional periodic metamaterial and an aperiodic rainbow metamaterial are investigated. Both metamaterial designs are modeled by the Spectral Element (SEM) method and the Finite Element (FEM) method. The simulated results are compared to each other and the results showed that the aperiodic rainbow metamaterial beam has extended stop-bands compared with the periodic one. Others results related to the rainbow effects, like slowing down the elastic waves are also presented.

## 2. Aperiodic Metamaterial Modeling

### 2.1 Beam Spectral Element

Base on the Euler-Bernoulli beam model, the homogeneous govern equation of a structural beam in the frequency domain can be expressed as Lee (2009):

$$EI\frac{d^4v}{dx^4} - \beta^4 v = 0, \tag{1}$$

where $v$ is the transversal displacement, $E$ is the Young's modulus, $I$ is the inertia moment, $A$ is the cross section area, and $\beta = \sqrt{\omega}(\rho A/EI)^{1/4}$. In order to introduce some damping into the system, a complex Young's modulus is used as $E_c = E(1+i\eta)$, where $\eta$ is the loss factor.

It can be shown that the forth-order Eq. (1) solution is obtained from particular solutions of two equations ($EId^2v/dx^2 + \beta^2 v = 0$ and $EId^2v/dx^2 - \beta^2 v = 0$), which demonstrates that the beam has two different propagation modes. Since the equations have constant coefficients, then the solutions are $v = ae^{-ikx}$, which on substituting into the equations gives the wavenumbers $k_1 = \pm\beta$ and $k_2 = \pm i\beta$. The internal transversal shear force and bending moment are given by:

$$M = EI\frac{\partial^2 v}{\partial x^2} = EIv'', \qquad V = -EI\frac{\partial^3 v}{\partial x^3} = -EIv''', \tag{2}$$

where $(')$ is the derivative related to the space. Based on the definition of displacements (transversal displacement $v$ and the slope $\phi = \partial v/\partial x$) and internal loads ($M$ and $V$) a length $L$ two nodes beam spectral element scheme is presented in Figure 1.

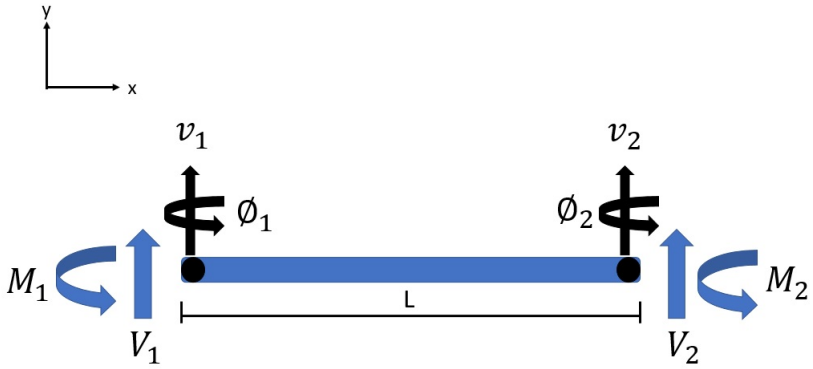


Figure 1. Two nodes beam spectral element scheme.

The solution of Eq. (1) for this two nodes beam spectral element of length $L$ can be written as:

$$v(x) = a_1e^{-ikx} + a_2e^{-kx} + a_3e^{-ik(L-x)} + a_4e^{-k(L-x)} = \mathbf{e}(x,\omega)\mathbf{a}, \tag{3}$$

where $\mathbf{e}(x,\omega) = [e^{-ikx}, e^{-kx}, e^{-ik(L-x)}, e^{-k(L-x)}]$ and $\mathbf{a} = \{a_1, a_2, a_3, a_4\}^T$. The nodal displacements and slopes can be relate to the displacement field by

$$\boldsymbol{d} = \begin{Bmatrix} v_1 \\ \phi_1 \\ v_2 \\ \phi_2 \end{Bmatrix} = \begin{Bmatrix} v(0) \\ v'(0) \\ v(L) \\ v'(L) \end{Bmatrix} \tag{4}$$

Substituting Eq. (3) on the right-hand side of Eq. (4) it has

$$\boldsymbol{d} = \begin{Bmatrix} \mathbf{e}(0,\omega) \\ \mathbf{e}'(0,\omega) \\ \mathbf{e}(L,\omega) \\ \mathbf{e}'(L,\omega) \end{Bmatrix} \mathbf{a} = \underbrace{\begin{bmatrix} 1 & 1 & e^{-ikL} & e^{-kL} \\ -ik & -k & ie^{-ikL}k & e^{-kL}k \\ e^{-ikL} & e^{-kL} & 1 & 1 \\ -ie^{-ikL}k & -e^{-kL}k & ik & k \end{bmatrix}}_{\mathbf{H_B}(\omega)} \mathbf{a} \tag{5}$$

The displacement field within the two nodes beam element can be represented in terms of the nodal DOFs vector $\boldsymbol{d}$ by eliminating the constant vector $\mathbf{a}$ from Eq. (3) by using Eq. (4), thus

$$v(x) = \underbrace{\mathbf{e}(x,\omega)\mathbf{H}_B^{-1}(\omega)}_{\mathbf{N}_B}\boldsymbol{d}, \tag{6}$$

where $\mathbf{N}_B$ is the function form matrix (Lee, 2009). The spectral nodal transverse shear forces and bending moments defined for the two nodes spectral beam element can be related to the corresponding forces and moments defined by the Eq. (2) as,

$$\boldsymbol{f} = \begin{Bmatrix} V_1 \\ M_1 \\ V_2 \\ M_2 \end{Bmatrix} = \begin{Bmatrix} -V(0) \\ -M(0) \\ V(L) \\ M(L) \end{Bmatrix} = \begin{Bmatrix} -v(0)''' \\ -v(0)'' \\ v(L)''' \\ v(L)'' \end{Bmatrix} \tag{7}$$

Substituting Eq. (6) into Eq. (2) and the results into the right-hand side of Eq. (7) gives

$$\boldsymbol{f} = EI \begin{bmatrix} -ik^3 & k^3 & ie^{-ikL}k^3 & -e^{-kL}k^3 \\ k^2 & -k^2 & e^{-ikL}k^2 & -e^{-kL}k^2 \\ ie^{-ikL}k^3 & -e^{-kL}k^3 & -ik^3 & k^3 \\ -e^{-ikL}k^2 & e^{-kL}k^2 & -k^2 & k^2 \end{bmatrix} \mathbf{a} = \mathbf{G}(\omega)\mathbf{a} \tag{8}$$

Substituting Eq. (5) in the Eq. (8) it has,

$$\boldsymbol{f} = \mathbf{G}(\omega)\mathbf{H}_B^{-1}(\omega)\mathbf{d} = \mathbf{S}_B(\omega)\mathbf{d} \tag{9}$$

where, $\mathbf{S}_B(\omega)$ is the dynamic stiffness Euler-Bernoulli beam spectral element matrix. Due to the matrix elements of $\mathbf{S}_B(\omega)$ are too extensive, they are not shown here, but can be obtained in the reference citations.

The transmittance of the metamaterial beam is defined as follows:

$$T(\omega) = \left| \frac{v_{1,1}(1)}{v_{2,N}(n)} \right| \tag{10}$$

where $N$ is the number of metamaterial beam unit-cells and $n$ is the number of frequency analyzed.

### 2.2 Local Resonator-Beam Coupling

The Local Resonators (LR) is modeled by a spring $k_0$ connected to a mass $m_0$. Base on the equilibrium equation of 1-DOF lumped system, the local resonator dynamic stiffness can be obtained as (Xiao *et al.*, 2021):

$$D_0 = \frac{(2\pi f)^2 m_0}{(f/f_0) - 1} \tag{11}$$

where $f_0 = (1/2\pi)\sqrt{k_0/m_0}$ is the resonance frequency of LR.

Figure 2 presents the local resonant metamaterial beam unit-cell, which consists of a spring-mass local resonator attached in the left-hand node of the structural beam of length $L_c$.

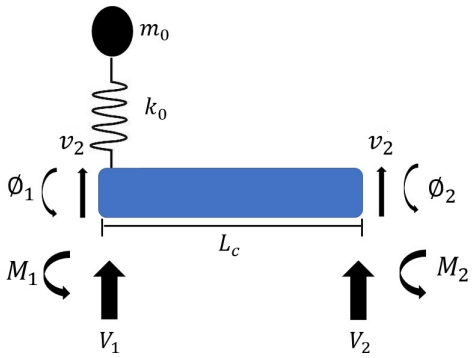


Figure 2. Local resonant metamaterial beam unit-cell scheme.

To obtained the metamaterial beam, first a unit-cell is obtained by assembling the LR dynamic stiffness into the left-hand node of the beam dynamic stiffness spectral element (or finite element). Then, the number of unit-cells desired ($N$) are assembled to obtain the global dynamic stiffness matrix of the entire beam metamaterial.

The graded local resonance in the metamaterial beam is similar to the proposed by Hua *et al.* (2021), where the first LR natural frequency ($\omega_1$) is chosen and the others LR natural frequencies vary according to an arithmetic progression of constant ratio ($\delta = (\omega_j - \omega_1)/[\omega_1(j-1)], j = 2, 3, \ldots, N$). The masses are identical, and the stiffness of each LR are calculated.

For the sake of conciseness the beam formulation by FEM will not be presented here, but it can be found in Petyt (2015).

## 3. SIMULATED RESULTS

For all simulated examples the metamaterial beam geometric parameters and material properties are summarized in Table 1.

Table 1. Simulated metamaterial beam geometric parameters and material properties.

| Geometry/Property | Value |
|---|---|
| Unit-cell length ($L_c$) | 0.1 m |
| Cross section area ($A$) | 4.0 x $10^{-5}$ $m^2$ |
| Number of unit-cells ($N$) | 6 |
| Young's modulus ($E$) | 210 x $10^9$ Pa |
| Mass density ($\rho$) | 7800 kg/$m^3$ |
| Structural damping ($\eta$) | 0.05 |
| Number of unit-cells $N$ | 6 |
| LR N. Frequencies [$f_0$] (Aperiodic) | [90 95 100 105 110 115] Hz |
| LR N. Frequencies [$f_0$] (Periodic) | 90 Hz |
| LR Masses $m_0$ | 0.02 kg |

In the first example a comparison between the SEM and FEM methods is evaluated for a bare beam (without LRs), a periodic metamaterial configured with 06 equal unit-cells (a LR with $f_0$ = 90 Hz and $m_0$ =0.02 kg attached to the left-hand node of a structural beam with $L_c$=0.1 m), and an aperiodic metamaterial configured with 06 different unit-cells (LRs with $f_0$ e $m_0$ as seen in Table 1 attached to the left-hand node of a structural beam with $L_c$=0.1 m). Figure 3 shows the transmittance of de metamaterial beams calculated by SEM and FEM with free-free (F-F) boundary conditions. The

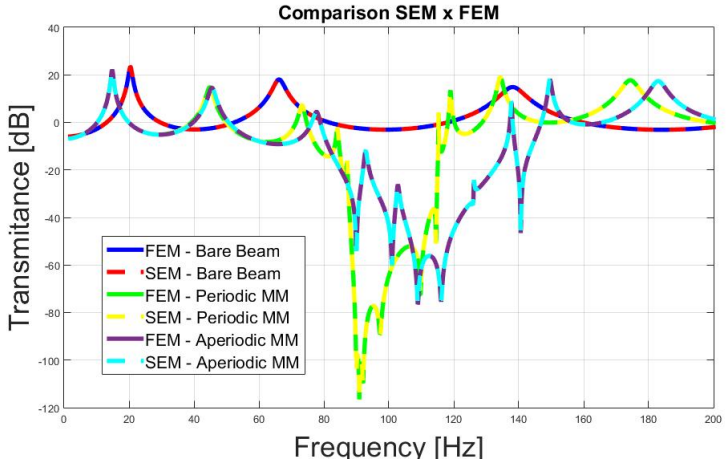


Figure 3. Transmitance calculated by SEM and FEM of a bare beam (without LRs), a periodic MM beam (06 equal LRs) and an aperiodic MM beam (06 different LRs).

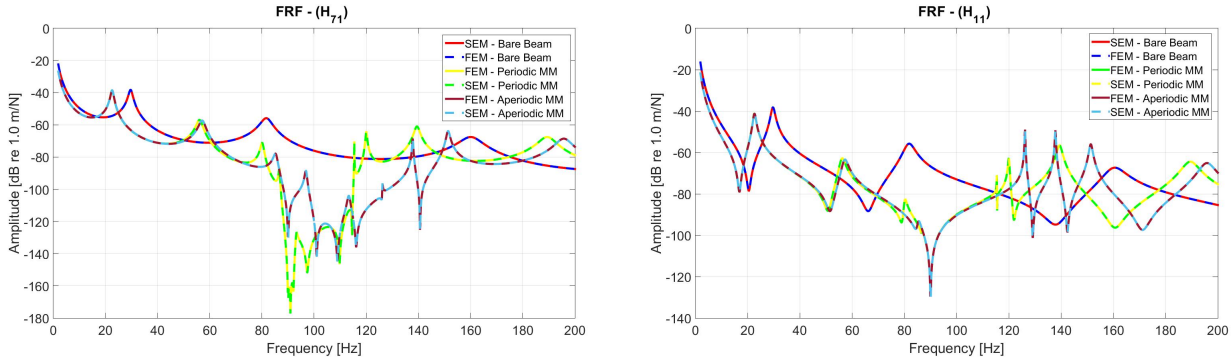


(*a*) (*b*)

Figure 4. Frequency response functions calculated by SEM and FEM of a bare beam (without LRs), a periodic MM beam (06 equal LRs), and an aperiodic MM beam (06 different LRs): (a) $H_{71}$; (b)$H_{11}$.

SEM metmaterial beam is modeled with 06 same dimension spectral elements, while the FEM metamaterial beam contain 36 equal finite elements (6 elements/unit-cell). For all cases, it can be seen a good agreement between the transmitances calculates by SEM and FEM. Also, the stop-band generated by the aperiodic metamaterial beam is larger than the periodic one. Frequency response functions (FRFs) at transfer point (Fig. 4a) and drive point (Fig. 4b) are calculated by SEM and FEM for the same metamaterial beams with F-F boundary conditions. The results obtained by both methods are good in agreement for all cases analyzed. Same evidence relate to the bandgaps generated by aperiodic and periodic metamaterial beams is confirmed here.

A local resonator parameters variation is performed for the aperiodic metamaterial using SEM method. The first parameter evaluated is the LR arithmetic progression ratio. By keeping all others parameters constants and varying $\delta = [1.0, 2.5, 5.0]$ the transmitance is calculated by SEM (Fig. 5). It can be seen that as the $\delta$ values increases the stop-band width also increases. The second parameter is the LR mass. By keeping all others parameters constants and varying

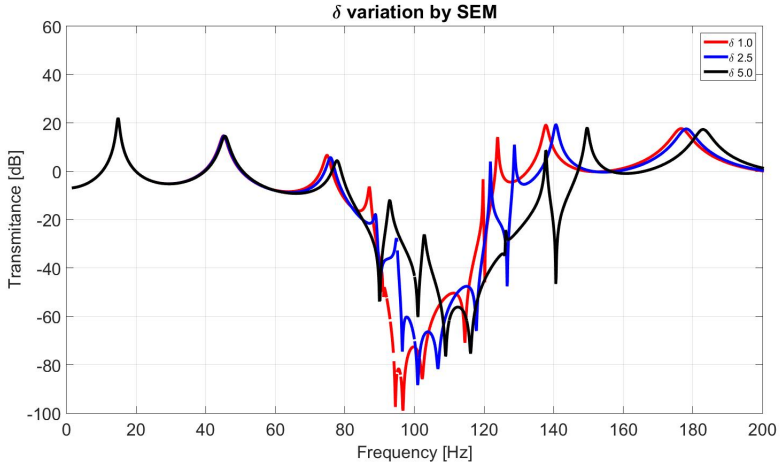


Figure 5. Transmitance of aperiodic metamaterial beam calculated by SEM with resonance frequency ratio $\delta = 1.0$, 2.5 and 5.

the 6 equal masses values as $m_0 = [0.01, 0.02, 0.04, 0.06]$, the transmitance is calculated by SEM (Fig. 6). For this case, it can be seen that stop-band width increases as the masses values in the LR increases.

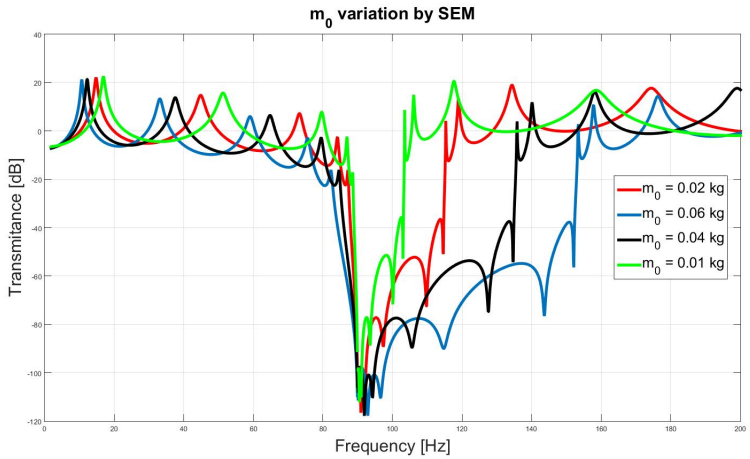


Figure 6. Transmitance of aperiodic metamaterial beam calculated by SEM with equal masses $m_0 = 0.01$, 0.02, 0.04 and 0.06 kg.

Performance to attenuate structural vibration with periodic and aperiodic metamaterial beam are evaluated. It was observed that varying the LR natural frequency for the periodic metamaterial, and the first LR natural frequency ($\omega_1$) of the arithmetic progression for the aperiodic metamaterial, the stop-band width and frequency band changes. To evaluated it the second natural frequency ($f_2 \approx 81.5$ Hz) of the bare beam was chosen as the vibration mode to be attenuated. For the periodic metamaterial the 06 equal LR natural frequency were varied and keeping all 6 LR masses $m_0 = 0.02$ kg. By trial-and-error the best values founded were all 6 LR frequencies $f_0 = 60$ or 70 Hz. Figure 7 shows the FRFs trasfer point $H_{71}$ and Transmitances calculated by SEM using these values. Figure 7a shows that both FRFs $H_{71}$ ($f_0 = 60$ and 70 Hz) presents significant attenuation at the vicinity of bare beam target vibration mode and shift it to a highest frequency.

However, for this case, the FRF $H_{71}$ with $f_0 = 70$ Hz seems to be more efficient, since it presents larger bandgap width and shifts target frequency farther. Similar behavior is observed for the Transmitances presented in Fig. 7b.

For the aperiodic metamaterial beam the first LR natural frequency ($\omega_1$) was varied, the 06 different LR natural frequencies are generated with the ratio $\delta = 5$, and all 6 LR masses $m_0 = 0.02$ kg. Same trial-and-error procedure was made for the aperiodic metamaterial beam, and the best values founded were $\omega_1 = 2\pi$ 60 and 70 Hz. Figure 8 shows the FRFs trasfer point $H_{71}$ and Transmitances calculated by SEM using these values. A behavior similar to the periodic case was observed as comparing between FRFs $H_{71}$ (Fig. 8a) and Transmitances (Fig. 8b) calculated with $\omega_1 = 60$ and 70 Hz. The aperiodic metamaterial beam presents also significant attenuation at the vicinity of the bare beam target vibration mode and shift it to a highest frequency. However, for both values of $\omega_1$ presents larger bandgap width and shifts target frequency farther.

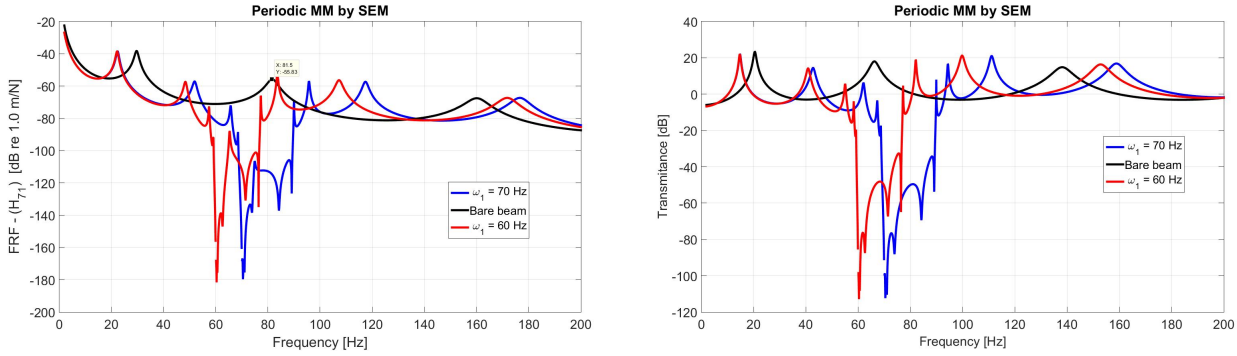


(*a*) (*b*)

Figure 7. Periodic metamaterial beam calculated by SEM using all 6 equal LRs with $f_0 = 60$ and 70 Hz, and $m_0 = 0.02$ kg: (a) FRF $H_{71}$; and (b) Transmitance.

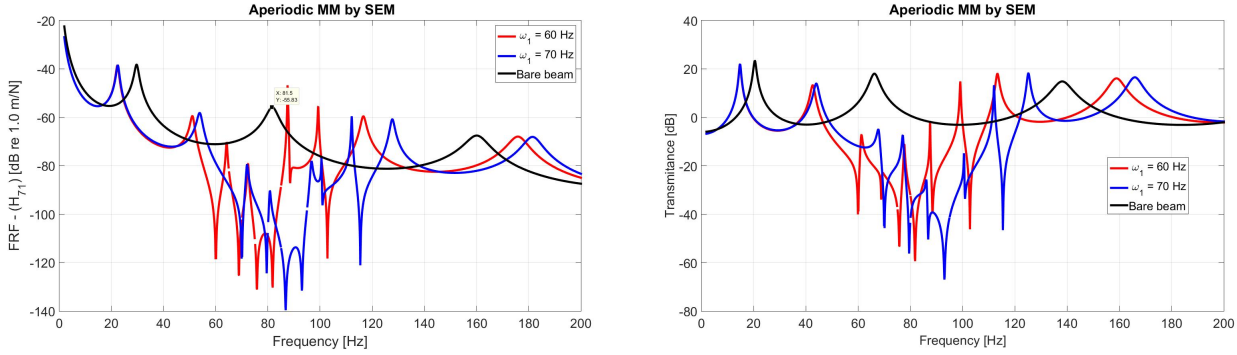


(*a*) (*b*)

Figure 8. Aperiodic metamaterial beam calculated by SEM using all 6 LR natural frequencies different with $\omega_1 = 2\pi$ 60 and 70 Hz, $\delta = 5$ and all 06 masses $m_0 = 0.02$ kg: (a) FRF $H_{71}$; and (b) Transmitance.

## 4. FINAL REMARKS

A rainbow metamaterial beam, consisting of aperiodic graded arrays of spring-mass resonators connected to an Euler-Bernoulli beam is presented. They are based on the rainbow trapping phenomena, which separates different frequency wave components and trap them in distinct positions in space. The rainbow metamaterial is composed by a graded array of loacal resonators attached transversely to a host longitudinal beam. The rainbow effects in a conventional periodic metamaterial and in an aperiodic metamaterial are investigated. Both metamaterial designs are modeled by the Spectral Element Method (SEM) method and verified by Finite Element Method (FEM). The simulated results are compared to each other and the results showed that the aperiodic rainbow metamaterial beam has extended stop-bands compared with the periodic one. Also, a parameters variation of the local resonators is performed and results related to the rainbow effects are presented and discussed. In the next steps other types of graded local resonance and effects of aperiodic metamaterial beam in its wave speed will be explored and evaluated. It should be noted that these results are preliminary and more investigation needs to be carried out with the aperiodic rainbow metamaterial in order to verify its performance limits.

## 5. ACKNOWLEDGEMENTS

The research leading to this article has been funded by FAPESP (Grant no. 2018/15894-0), CAPES (Finance Code 001) and CNPq (Grant no. 313620/2018). The support of DMC-FEM- UNICAMP are also gratefully acknowledged

## 6. REFERENCES

Assis, G., Beli, D., Jr., E.M., Camino, J., Dos Santos, J. and Arruda, J.F., 2019. "Computing the complex wave and dynamic behavior of one-dimensional phononic systems using a state-space formulation". *International Journal of Mechanical Sciences*, Vol. 163, p. 105088. doi:10.1016/j.ijmecsci.2019.105088.

Banerjee, A., 2021. "Flexural waves in graded metabeam lattice". *Physics Letters A*, Vol. 388, p. 127057. doi:10.1016/j.physleta.2020.127057.

Brennan, M.J., 1997. "Characteristics of a wideband vibration neutralizer". *Noise Control Engineering Journal*, Vol. 45, No. 5, pp. 201–207. doi:10.3397/1.2828441.

D'Alessandro, L., Krushynska, A.O.., Ardito, R., Pugno, N.M. and Corigliano, A., 2020. "A design strategy to match the band gap of periodic and aperiodic metamaterials". *Scientific Reports*, Vol. 10, p. 16403. doi:10.1038/s41598-020-73299-3.

Fabro, A., Beli, D., Ferguson, N., Arruda, J. and Mace, B., 2021. "Wave and vibration analysis of elastic metamaterial and phononic crystal beams with slowly varying properties". *Wave Motion*, Vol. 103, p. 102728. doi:10.1016/j.wavemoti.2021.102728.

Fang, N., Xi, D., Xu, J., Ambati, M., Srituravanich, W., Sun, C. and Zhang, X., 2006. "Ultrasonic met-amaterials with negative modulus". *Nature materials*, Vol. 452, No. 5. doi:10.1038/nmat1644.

Goto, A.M., Nóbrega, E.D., Pereira, F.N. and Dos Santos, J.M.C., 2020. "Numerical and experimental investigation of phononic crystals via wave-based higher-order rod models". *International Journal of Mechanical Sciences*, Vol. 105776, No. 181. doi:10.1016/j.ijmecsci.2020.105776.

Hua, G., Austin, A.C.M., Sorokin, V. and Tang, L., 2021. "Metamaterial beam with graded local resonators for broadband vibration suppression". *Mechanical Systems and Signal Processing*, Vol. 146, p. 106982. doi:10.1016/j.ymssp.2020.106982.

Lee, U., 2009. *Spectral Element Method in Structural Dynamics*. Wiley. ISBN 9780470823750.

Liu, Z., Zhang, X., Mao, Y., Zhu, Y., Yang, Z., Chan, C. and Sheng, P., 2000. "Locally resonant sonic materials". *Science*, Vol. 289, pp. 1734–1736. doi:http://dx.doi.org/10.1126/science.289.5485.1734.

Meng, H., Chronopoulos, D., Fabro, A., Elmadih, W. and d, I.M., 2020. "Rainbow metamaterials for broadband multi-frequency vibration attenuation: Numerical analysis and experimental validation". *Journal of Sound and Vibration*, Vol. 465, p. 115005. doi:10.1016/j.jsv.2019.115005.

Miranda, E., Nobrega, E., Ferreira, A. and Dos Santos, J., 2019. "Flexural wave band gaps in a multi-resonator elastic metamaterial plate using kirchhoff-love theory". *Mechanical Systems and Signal Processing*, Vol. 116, pp. 480–504. doi:10.1016/j.ymssp.2018.06.059.

Nobrega, E.D., Gautier, F., Pelat, A. and Dos Santos, J., 2016. "Vibration band gaps for elastic metamaterial rods using wave finite element method". *Mechanical Systems and Signal Processing*, Vol. 79, pp. 192–202. doi:10.1016/j.ymssp.2016.02.059.

Pendry, J., 2020. "Negative refraction makes a perfect lens". *Physical Review Letters*, Vol. 85, pp. 3966–3969. doi:10.1103/PhysRevLett.85.3966.

Petyt, M., 2015. *Introduction to Finite Element Vibration Analysis*. Cambridge University Press.

Xiao, Y., Wang, S., Li, Y. and Wen, J., 2021. "Closed-form bandgap design formulas for beam-type metastructures". *Mechanical Systems and Signal Processing*, Vol. 159, p. 107777. ISSN 0022-460X. doi:10.1016/j.ymssp.2021.107777.

## 7. RESPONSIBILITY NOTICE

The authors are solely responsible for the printed material included in this paper.